

Neutral Particle Analysis on ITER: Present Status and Prospects

V.I. Afanasyev, F.V. Chernyshev, A.I. Kislyakov, S.S. Kozlovski^a, B.V. Lyublin^b, M.I. Mironov, A.D. Melnik, V.G. Nesenevich, M.P. Petrov, S.Ya. Petrov

A.F. Ioffe Physical Technical Institute, 26 Polytekhnicheskaya st, St.Petersburg, 194021, Russian Federation, fax: (812)2971017, tel: (812)2976096, val@npd.ioffe.ru

^aSt.Petersburg State Politechnical University, 29 Polytehnicheskaya st, St.Petersburg, 195251, Russia Federation

^bD.V. Efremov Institute of Electrophysical Apparatus, 3 Doroga na Metallostroy, St. Petersburg, 196641, Russian Federation

Keywords: ITER diagnostics system, neutrals, thermal ions, fast particles

Abstract. In this report we present the abilities of the Neutral Particle Analysis (NPA) measurements for ITER steady-state (SS) operation scenario in respect to the main objective of the NPA diagnostic on ITER, which is to measure the DT fuel composition of the fusion plasma. We analyze the physical basis for measuring of the neutral particle fluxes emitted by ITER plasma and consider the possible mechanisms of the neutralization of the hydrogen and helium ions in the thermal and supra-thermal energy ranges. Numerical simulation results of the neutral fluxes produced by the neutralization processes of the bulk thermal deuterium and tritium ions, Neutral Heating Beam particles and “knock-on” deuterium and tritium ions are presented. Integration of NPA tandem consisting of Low Energy Neutral Particle Analyzer (LENPA) and High Energy Neutral Particle Analyzer (HENPA) is described. The analyzers provide the measurements in thermal (10 – 200 keV) and supra-thermal (0.1 – 4 MeV) ranges respectively. Calculation of the counting rates in the analyzer energy channels shows that the NPA system will be able to measure D/T ratio both in ITER plasma core ($r < 0.4a$) by measuring of the neutralized “knock-on” deuterons and tritons and in plasma medium region ($r > 0.4a$) by measuring of the neutralized thermal deuterons and tritons.

1. Introduction

The main objective of the NPA diagnostic on ITER is to measure the DT fuel composition of the fusion plasma. It can be provided on the basis of measurement of the neutralized fluxes of the corresponding hydrogen ions, namely protons, deuterons and tritons [1]. Below we present the physical basis of this diagnostic and the expected results.

2. Physical Basis for Modeling of Neutral Particle Fluxes on ITER

The following base points should be clarified for a modeling of the neutral fluxes in ITER plasma:

- Origin of the populations of ions for ITER specific plasma parameters;
- Neutralization target for the ions in thermal and supra-thermal energy ranges;
- NPA diagnostic layout for the detection of the resulted neutral fluxes entering the NPA system.

If these points are known, a number of the neutral atoms $\phi(E)$ emerging from a unit volume of the plasma with energy E can be defined as:

$$\phi_{H^0, D^0, T^0, He^0}(E) = n_{p,d,t,\alpha} f_{p,d,t,\alpha}(E) \sum_k n_k \langle \sigma v \rangle_k \quad (1)$$

where $n_{p,d,t,\alpha}$ and $f_{p,d,t,\alpha}$ are the densities and energy distribution functions of the ions (protons, deuterons, tritons or alphas), the summation is made over the neutralization targets of the density n_k and the neutralization rate $\langle \sigma v \rangle_k$.

Finally, the flux of atoms $\Gamma(E)$ emitted by the plasma along the line of sight of the NPA system L can be expressed as:

$$\Gamma_{H^0, D^0, T^0, He^0}(E) = \int_L \phi_{H^0, D^0, T^0, He^0}(E, l) \mu(E, l) dl \quad (2)$$

Here $\mu(E, l)$ is the plasma transparency for the outgoing atomic flux defined by the reionization probability. The transparency can be rather small for the thermal atoms in ITER plasma (~ 0.1 or less depending on the energy), but for supra-thermal atoms the attenuation is low and, hence the transparency for this case ~ 1 .

It is seen from Equations (1) and (2) that the atomic fluxes provide the information on the main component of the plasma, namely on the hydrogen isotope ions. The flux of atoms of each particular isotope is a function of the density of this isotope, assuring by this a base for measuring the isotope ratio of the plasma ion component. It is also important that the flux of atoms of a certain energy emitted by plasma has a maximum probability to be produced at a certain distance from the plasma edge and this distance increases with increasing of the energy of atoms. This creates the possibility of determining the plasma hydrogen ion isotope ratio as a function of the plasma radius from the energy dependent measurements of the flux ratio [1].

2.1. Reference Plasma Parameters and NPA Diagnostic Layout

For modeling we used the equilibrium and the plasma profiles of the steady state operation scenario of ITER (S4) [2] with the main parameters as follows: plasma density $n_{e0} = 0.7 \times 10^{20} \text{ m}^{-3}$, central ion temperature $T_{i0} = 33 \text{ keV}$, central electron temperature $T_{e0} = 30 \text{ keV}$, plasma effective charge $Z_{\text{eff}} = 1.7$, hydrogen isotope ratio $n_D/n_T = 1$, density of helium ash $n_{He^{2+}}/n_e = 7.5 \%$, density of the main light impurities $n_{Be^{4+}}/n_e = n_{C^{6+}}/n_e = 1 \%$, total power of the heating neutral beam $P_{\text{HNBtotal}}(D^0, 1 \text{ MeV}) = 33 \text{ MW}$. It is also assumed the use of the diagnostic neutral beam with the power $P_{\text{DNB}}(D^0, 200 \text{ keV}) = 5 \text{ MW}$. NPA Diagnostic layout and its location in ITER relatively to the beams are shown in Fig.21 of section 4, where the integration of the NPA system into ITER environment is described in details.

2.2. Energy and Space Distribution Function of the Ions

For the thermal part of the calculations we assumed the Maxwellian energy and the isotropic space distributions of the bulk ions. The distribution functions of the Heating Neutral Beam (HNB) and Diagnostic Neutral Beam (DNB) and contribution of the beam particles into NPA measurements are calculated with use of DRIFT part of the HYBRID code [3, 4], which is a pure Orbit Following Monte Carlo code. No acceleration technique, such as MAPPING part of the HYBRID or acceleration of Coulomb scattering process etc. was applied in the present calculations.

To estimate the contribution of the fusion alphas and effects induced by the alphas into NPA measurements we have to use the results presented in [5]. It is considered that the alphas have no losses and their behavior is determined according to the predictions of the classical theory. In presence of the high energy alphas, a very specific population of D^+ and T^+ ions in MeV energy range can be produced. Those are so-called “knock-on” D^+ and T^+ ions [6]. These particles appear as a result of the close elastic collisions of the fusion alphas with the thermal D^+ and T^+ ions. In the present calculations we scaled the magnitude of these energy tails according to the change of the local plasma parameters.

2.3. Density of the Neutralization Targets

A flux of the neutral hydrogen (deuterium, tritium) atoms is produced in ITER plasma by three neutralization processes: 1) charge exchange with the background hydrogen isotope neutrals, 2) radiative recombination of the protons (deuterons, tritons) with the electrons and 3) electron capture from the hydrogen-like impurity ions. The neutralization rate from the Equation (2) can be defined as:

$$\sum_k n_k \langle \sigma \nu \rangle_k = \sum_i n_{0,i} \langle \sigma \nu \rangle_{CX,i} + \sum_j n_{[H]imp,j} \langle \sigma \nu \rangle_{CX[H]imp,j} + n_e \langle \sigma \nu \rangle_{rec} \quad (3)$$

where n_0 is the density of the background hydrogen isotope neutrals D^0 and T^0 , $n_{[H]imp}$ are the densities of the hydrogen-like impurity ions C^{5+} and Be^{3+} (main low-Z impurities in ITER) and helium ash ions He^+ , n_e is the electron density, $\langle \sigma \nu \rangle_{CX}$, $\langle \sigma \nu \rangle_{CX[H]imp}$ and $\langle \sigma \nu \rangle_{rec}$, are the rate coefficients for the corresponding charge exchange and recombination processes. The ratio between these neutralization processes varies depending on the particle energy and its location in the plasma (see section 3).

Density of the background hydrogen neutrals is usually derived from the numerical codes. These codes evaluate a propagation of the neutrals from the plasma edge into the plasma center for the known radial distributions of the density and temperature of the ions and electrons and the specified value of the edge neutral influx, taking into account all of the elementary atomic processes. For modeling of the radial neutral distributions we used a part of the DOUBLE-MC code.

Densities of the hydrogen like impurity ions were calculated with use of the ZIMPUR impurity code [7]. Except for the most periphery of ITER plasma this code gives the impurity densities close to the values estimated in the frame of the Coronal equilibrium model and confirms a weak role of the impurity transport processes for these calculations [8]. Therefore the helium ash density of He^+ ions was also calculated from the Coronal equilibrium model. The results of the neutralization target density calculations are shown in Fig.1.

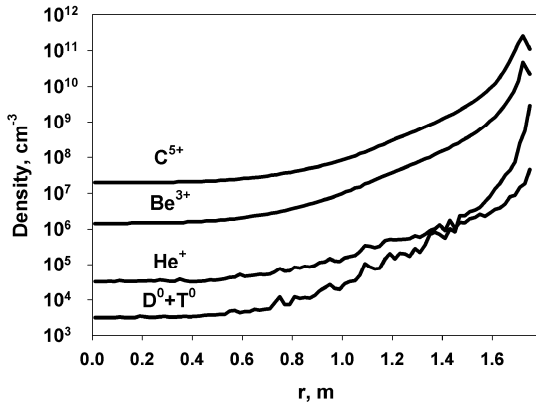


Fig.1. Radial distributions of the main neutralization targets for D^+ and T^+ ions in ITER plasma.

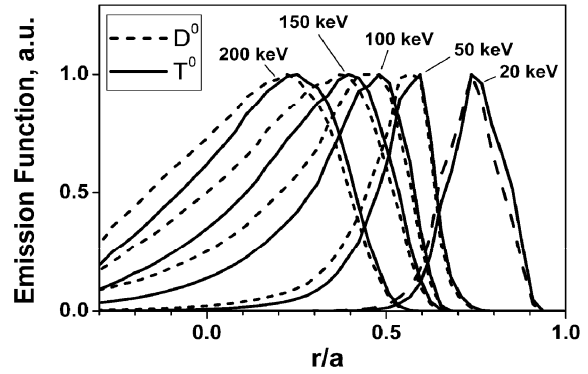


Fig.2. Emission functions for D^0 and T^0 atoms of the thermal range energies versus ITER plasma minor radius.

3. The Results of Neutral Particle Fluxes Modeling

DOUBLE-MC code developed in the Ioffe Institute has been used to model the neutral fluxes in ITER plasma. The code is a Monte-Carlo version of the analytic method described in [9]. Inputs of the DOUBLE are as follows: the plasma density (including the main light impurities) and temperature radial profiles, the map of magnetic surfaces and the observation line geometry. The code provides simulation of the multi-component plasma and gives the following outputs: the radial neutral (H^0 , D^0 and T^0) distributions in plasma, the energy spectra of the emitted neutral fluxes and the dependence of the emissivity functions of the neutral fluxes both on the energy and plasma minor radius. Below we present the results of the neutral flux modeling for the thermal and supra-thermal energy ranges in ITER. The former can be used to study the bulk plasma ion component, whereas the latter is suitable for the study of the high energy ions (such as D^+ , T^+ ions or alphas of the MeV energy range) generated by an auxiliary heating or produced by the fusion reactions in plasma.

3.1. Thermal Energy Range

The calculated emission functions for D^0 and T^0 atoms related to the thermal ions of the different energies versus the plasma minor radius are presented in Fig.2. These functions are proportional to the probabilities of the neutral atoms to escape plasma from the certain radius. It can be seen that atoms having energy $E > 150$ keV are emitted by the central plasma region within $r < 0.4a$ (a – minor radius). Lower energy atoms are emitted by the outer part of plasma.

Fig.3 shows the radial dependence of the neutralization rates for D^+ and T^+ ions due to the different neutralization donors. Vertical dashed lines in the figure correspond to the position of the emission function maximums of the different energies given in Fig.6. It is seen that for the central region of plasma the neutralization of the deuterium and tritium ions of the thermal energies range occurs mainly due to the charge exchange reaction with He^+ ions and radiative recombination with electrons. Near plasma periphery the charge exchange reaction on D^0 and T^0 neutrals becomes more important.

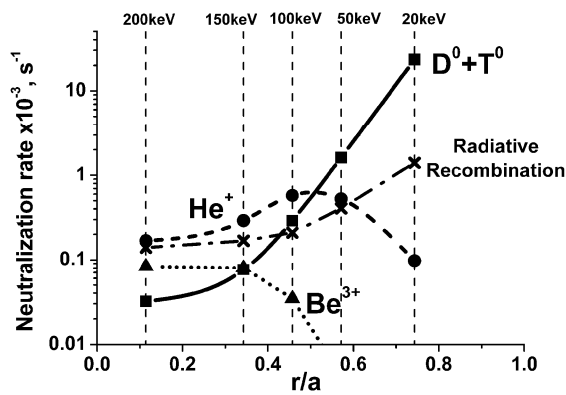


Fig.3. Neutralization rate of the thermal D^+ and T^+ ions versus energy for different reactions.

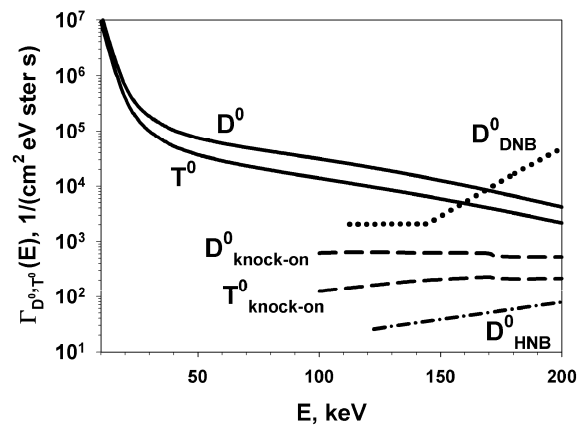


Fig.4. Energy spectra of D^0 and T^0 atoms emitted by ITER plasma in the thermal energy range.

The calculated neutral fluxes of D^0 and T^0 atoms emitted by ITER plasma in the thermal energy range 10 – 200 keV into the NPA system (see Equation (2)) are presented in Fig.4. The contributions of the neutralized knock-on ions ($D^0_{\text{knock-on}}$ and $T^0_{\text{knock-on}}$) and the neutralized ions originating from the heating (D^0_{HNB}) and diagnostic (D^0_{DNB}) beams are also shown in the figure. It is seen that a reliable D/T ratio measurement is possible if the neutral fluxes of D^0 and T^0 atoms are measured in the energy range up to $\sim 100 - 110$ keV only, where the neutral energy spectra are free of the non-thermal particles. In this case the measurements are limited by the plasma area $r > 0.4a$. In the absence of the diagnostic beam, the NPA measurements can be extended up to the energy 200 keV where the Maxwellian energy distribution is still not disturbed by the heating beam and knock-on ions. It makes possible to get the information about the hydrogen isotope ratio from the plasma area close to the core ($r \sim 0.25$).

3.2. Supra-Thermal Energy Range

Energy dependence of the neutralization rates of the fast hydrogen isotope ions is shown in Fig.5. In the relatively low energy range $E < 1$ MeV it is necessary to take into account all of the neutralization reactions: electron capture from He^+ , Be^{3+} , C^{5+} ions and radiative recombination. For the energies $E > 1.2$ MeV the latter two processes become dominant. Note that even in the pure plasma the radiative recombination can produce a significant neutralization effect alone.

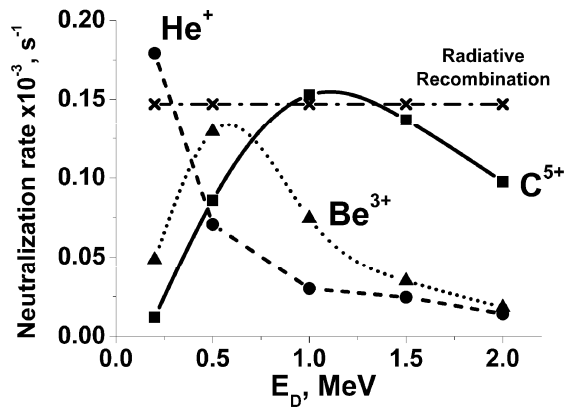


Fig.5. Neutralization rate of the fast D^+ ions versus energy for the different reactions.

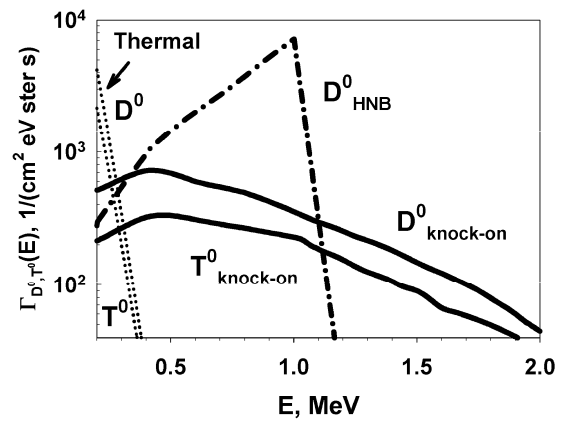


Fig.6. Energy spectra of D^0 and T^0 atoms emitted by ITER plasma in the supra-thermal energy range.

1 Fig.6 presents the calculated neutral fluxes of D^0 and T^0 atoms emitted by ITER plasma in
 2 the supra-thermal energy range into the NPA system. It is seen that the knock-on deuterium
 3 flux is significantly disturbed by the heating beam particles in the energy range $E < 1.2$ MeV.
 4 The knock-on tritium flux is also mixed with the thermal tail of the energy spectrum in the
 5 range $E \sim 250 - 350$ keV. So the supra-thermal energy ranges $E_D > 1.2$ MeV for the
 6 deuterium and $E_T > 0.4$ MeV for tritium neutral fluxes are appeared to be the most reliable for
 7 the accurate D/T isotope measurements in the plasma core. It is clear that these measurements
 8 are integrated over the plasma core where fusion alphas are confined.

4. Modeling of NPA parameters

12 The energy parameters and the detection efficiency were evaluated with use of the
 13 especially designed computer code, which simulates the electromagnetic dispersion system of
 14 the analyzers and provides the ion trajectory calculations [10]. The energy dependences of the
 15 detection efficiency for different particle species are presented in Fig.7a and Fig.7b for
 16 LENPA and HENPA, respectively.

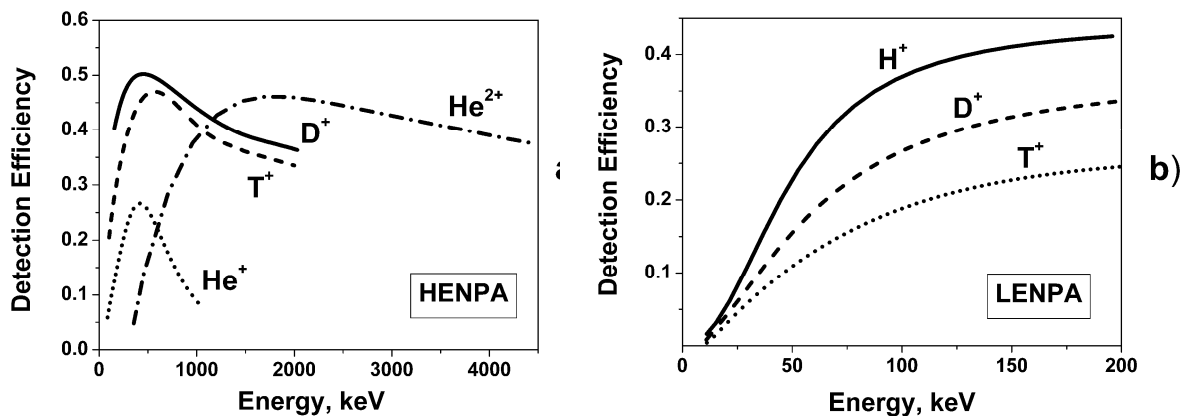


Fig.7. Calculated detection efficiency of H^0 , D^0 , T^0 and $4He^0$ atoms for HENPA (a) and LENPA (b) versus the atomic energy.

17 Calculated relative energy widths of HENPA channels $\Delta E_n/E_n$ are equal to $(5 - 3) \%$
 18 changing with increasing of the channel energy E_n (average particle energy of the channel).
 19 For LENPA those values are equal to $(30 - 5) \%$. These expected parameters of the devices

1 were taken into account below for the evaluation of the NPA counting rates produced by the
2 different neutral fluxes emitted from plasma.

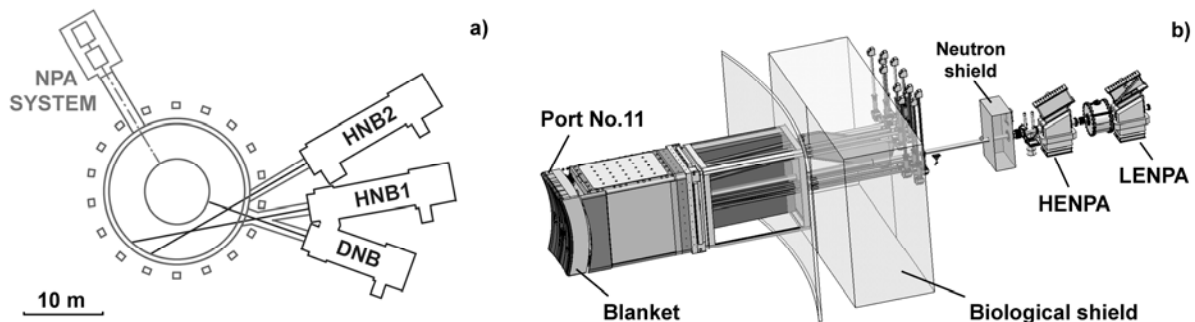
3 After manufacturing and assembling it is implied to calibrate both instruments with use of
4 the atomic beams. LENPA will be calibrated in keV-energy range with the use of the beam
5 generated by the hydrogen/deuterium ion source. HENPA will be calibrated in sub-MeV and
6 MeV-energy ranges with the use of the beam generated by the cyclotron accelerator. The
7 main aims of calibration are to measure experimentally the detection efficiencies, the energy
8 widths of the channels and the mass suppression coefficients of the analyzers.

9 10 **5. NPA Tandem. Integration of NPA system into ITER Environment.**

11
12 The designing of the NPA system has shown that it is very difficult to provide the
13 simultaneous measurements in the full 10 keV – 4 MeV energy range with the use of only one
14 instrument. To satisfy the main NPA objectives and the accuracy requirements it is reasonable
15 to split the energy range into the thermal and supra-thermal parts and to have two
16 corresponding different analyzers (tandem) covering the corresponding ranges.

17 The NPA tandem consists of High Energy Neutral Particle Analyzer (HENPA) for 0.1 –
18 4.0 MeV energy range and Low Energy Neutral Particle Analyzer (LENPA) for 10 – 200 keV
19 energy range. HENPA and LENPA both are viewing plasma along the main radius close to
20 the equatorial plane of the torus through the same straight vacuum beam line. The beam line
21 has two special opening windows of the same diameter 20 mm at the entrance of the NPA
22 system. Both analyzers can operate in parallel because LENPA is shifted horizontally to
23 ensure the independent line of sight.

24 The NPA tandem will be located at the ITER vacuum vessel equatorial port No.11 [11] and
25 incorporated into the secondary vacuum container together with the X-ray Crystal
26 Spectroscopy (India), the Vacuum Ultra-Violet spectrometer (Korea) and the Reflectometry
27 (USA). The general layout of the port No.11 and integration of the diagnostic equipment into
28 the ITER environment are presented in the Fig.8.



33 Fig.8. a) Location of NPA System in ITER (top view). HNB1 and HNB2 are Heating Neutral
34 Beam Injectors, DNB is Diagnostic Neutral Injector; b) General layout of ITER port No.11.

35 The distance from the plasma edge to HENPA stripping foil is $L_1 = 12$ m, to LENPA
36 stripping foil is $L_2 = 14$ m. This geometry provides the necessary acceptance angles of
37 HENPA and LENPA which are equal to $\omega_{\text{HENPA}} = S/L_1^2 = 2.2 \times 10^{-6}$ sterad and $\omega_{\text{LENPA}} = 1.6 \times$
38 10^{-6} sterad, respectively (S is the area of the stripping foils).

39 The requirements to the NPAs are as follows: 1) Simultaneous detection of the neutral
40 fluxes of different mass species (all three hydrogen isotopes H^+ , D^+ , T^+ for LENPA and D^+
41 $, T^+$, $4He^+$, $4He^{2+}$ for HENPA; 2) High mass resolution (suppression of the neighbour masses
 $\sim 10^{-3}$); 3) High detection efficiency of the neutral atoms (0.1 – 0.5); 4) Low sensitivity to the
neutron-gamma radiation ($10^{-6} - 10^{-7}$ pulses/neutron).

1 The requirements have been met by the following means: 1) usage of a thin carbon
 2 diamond-like foil (DLC foil, thickness $\sim 100 \text{ \AA}$, diameter 20 mm) for the stripping of the
 3 atoms [12], 2) additional acceleration $\sim +100 \text{ kV}$ of the secondary ions after stripping (in
 4 LENPA only), 3) optimization of the electromagnet dispersion systems of $E \parallel B$ type, which
 5 separate particles by the energy and mass, and 4) development of the particle detectors having
 6 a very low neutron-gamma radiation sensitivity (scintillation detectors with a scintillator
 7 thickness of the micron range).

8 The prototype of LENPA (ISEP NPA [13]) and prototype of HENPA (GEMMA NPA [14])
 9 were successfully tested and are under use on JET. GEMMA NPA has been effectively used
 10 also in JT-60U [15, 16] and TFTR DT experiments [17].

11 6. Expected NPAs Count Rates

12 Summarizing the results of the neutral fluxes modelling (section 3) and the calculated data
 13 for the NPAs parameters (sections 4) we can estimate the corresponding particle count rates
 14 and the noise background in the NPA energy channels. The count rate in a particular energy
 15 channel with energy E can be defined as:

$$16 N(E) = \Gamma(E)\Delta E\omega S / (4\pi\alpha(E)) \quad (7)$$

17 where $\Gamma(E)$ is the neutral flux emitted by plasma either in the thermal or supra thermal energy
 18 ranges (see Equation 2), ΔE is the energy width of the channel, ω is the NPA acceptance
 19 angle, S is the plasma area viewed by the NPA, $\alpha(E)$ is the detection efficiency for the
 20 neutrals.
 21
 22

23 Fig.9 shows the count rates when detecting the thermal D^0 and T^0 atoms by LENPA versus
 24 the atom energy in ITER operation scenario S4 (see section 2.1) when n_D/n_T isotope ratio is
 25 equal to 1. For energies $E < 100 \text{ keV}$ where non thermal particles do not disturb the
 26 Maxwellian spectra (see section 3.1), the count rates exceeds 1 kHz. This provides better than
 27 10 % of the statistical accuracy for the time window 100 ms and a very good signal to
 28 neutron-gamma noise ratio ~ 100 . As have been mentioned above in this case we have the
 29 information about the D/T isotope ratio from the outer plasma area $r > 0.4a$.

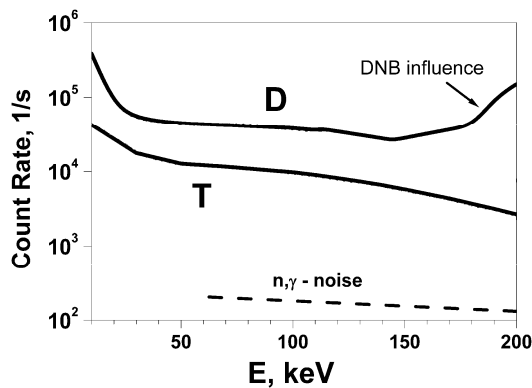


Fig.9. Energy dependence of the expected D^0 and T^0 counting rates in LENPA.

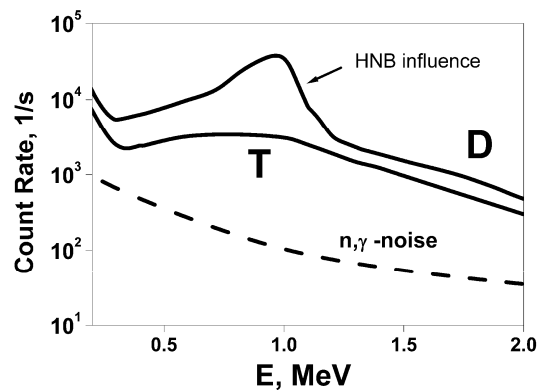


Fig.10. Energy dependence of the expected D^0 and T^0 counting rates in HENPA.

30 The energy dependencies of the count rates of the supra-thermal D^0 and T^0 atoms expected
 31 to be detected by HENPA are presented in Fig.10. For the proposed energy ranges ($E_D > 1.2$
 32 MeV and $E_T > 0.4 \text{ MeV}$, see section 3.2) where the knock-on spectra are not disturbed by the
 33 heating beam and thermal particle tails, the count rates reach the value 0.3 – 3 kHz. We can
 34 see again that it is possible to provide the D/T isotope measurements with 10 % of the

1 statistical accuracy for the time window 100 ms to satisfy the ITER requirements. In this case
2 the signal to neutron-gamma noise ratio is also expected to be acceptable ~ 10 . Obviously
3 these measurements correspond to the inner plasma area ($r < 0.4a$) where the fusion alphas are
4 confined and produce the knock-on ions.

6 7. Conclusions

8 We can state that the tandem of two advanced instruments (LENPA and HENPA) have
9 being developed at the Ioffe Institute for the use on ITER meet the following requirements: a)
10 detection of the neutral fluxes of all three hydrogen isotopes (H, D, T) in the thermal energy
11 range (10 - 200 keV for LENPA) and b) detection of the neutral fluxes originating from the D
12 and T knock-on ions in the supra-thermal energy range (0.1 – 2 MeV for HENPA) with the
13 high detection efficiency and the acceptable signal to noise ratio. It is achieved by using of
14 thin DLC foils (~ 10 nm) for the stripping, additional acceleration (by ~ 100 kV) of the
15 secondary ions (in LENPA), optimization of the NPA dispersion systems and development of
16 the particle detectors having the very low neutron-gamma sensitivity (scintillation detectors
17 with scintillator thickness of the micron range). Specially developed numerical codes have
18 been used for the simulation of the expected NPA signals. Calculations show that the NPA
19 system will be able to measure D/T fuel ratio both in the core and outer region of ITER
20 plasma with the required statistical accuracy and time resolution.

21 22 References:

- 23
24 [1]. A.I. Kislyakov, M.P. Petrov and E.V. Suvorkin, Plasma Phys. Control Fusion, 43,
25 (2001) 1175.
26 [2]. ITER Technical Basis, Chapter 4, p.11, <http://www.iter.org/pdfs/PDD4.pdf>.
27 [3]. S.V. Konovalov et al, in Proc. IAEA Technical Committee Meeting on Alpha Particles
28 in Fusion Research, Kiev, USSR, 1989, V1, p.107.
29 [4]. S.V. Konovalov et al, JAERI-Research 94-033 (1994).
30 [5]. L. Ballabio, G. Gorini, J. Kallne, Phys. Rev. E 55 (1997) 3358-3368.
31 [6]. D. Ryutov, Phys. Scr. 45 (1992) 153-158.
32 [7]. V.M. Leonov and V.E. Zhogolev, Plasma Phys. Control. Fusion 47 (2005) 903–918.
33 [8]. V.I. Afanasyev, M.I. Mironov, S.V. Konovalov et al, AIP Conf. Proc., v.988, 2008,
34 pp.177-184.
35 [9]. Yu.N. Dnestrovskij, S.E. Lysenko, A.I. Kislyakov, Nucl. Fusion 19 (1979) 293-299.
36 [10]. V.I. Afanasiev et al, Rev. Sci. Instrum. 73 (2003) 2338-2352.
37 [11]. V.I. Afanasiev et al, Plasma Devices and Operations 12 (2004) 209-215.
38 [12]. V.Kh. Liechtenstein et.al, Nucl. Instr. and Meth. A 480 (2002) 185-190.
39 [13]. V.I. Afanasiev et al, Rev. Sci. Instrum. 73 (2003) 2338-2352.
40 [14]. M.P. Petrov et al, in Proc. Conf. on Plasma Physics, Innsbruck, 1992, vol.16C, Part II,
41 p.1031.
42 [15]. Y. Kusama, M.Nemoto, M.Satoh et al, Rev. Sci. Instrum., 66 (1995) 339-341.
43 [16]. V.I. Afanassiev, Y.Kusama, M.Nemoto et al, Plasma Phys. Control. Fusion 39 (1997)
44 1509-1524.
45 [17]. S.S. Medley et al, Rev. Sci. Instrum. 67 (1996) 3122-3135.
46